Structure
Article

Phosphorylation-Induced Conformational Switching of CPI-17 Produces a Potent Myosin Phosphatase Inhibitor

Masumi Eto,[1,*] Toshio Kitazawa,[2] Fumiko Matsuzawa,[3] Sei-ichi Aikawa,[3] Jason A. Kirkbride,[1] Noriyoshi Isozumi,[4] Yumi Nishimura,[4] David L. Brautigan,[5] and Shin-ya Ohki[4,*]
[1]Department of Molecular Physiology and Biophysics, Thomas Jefferson University, 1020 Locust Street, Philadelphia, PA 19107, USA
[2]Boston Biomedical Research Institute, 64 Grove Street, Watertown, MA 02472, USA
[3]Department of Clinical Genetics, Tokyo Metropolitan Institute of Medical Science, Honkomagome 3-18-22, Bunkyo-ku, Tokyo 113-8613, Japan
[4]Center for Nano Materials and Technology (CNMT), Japan Advanced Institute of Science and Technology (JAIST), 1-1 Asahidai, Tatsunokuchi, Ishikawa, 923-1292, Japan
[5]Center for Cell Signaling, University of Virginia School of Medicine, 1400 Jefferson Park Avenue, Charlottesville, VA 22908, USA
*Correspondence: masumi.eto@jefferson.edu (M.E.), shinya-o@jaist.ac.jp (S.-y.O.)
DOI 10.1016/j.str.2007.10.014

SUMMARY

Phosphorylation of endogenous inhibitor proteins for type-1 Ser/Thr phosphatase (PP1) provides a mechanism for reciprocal coordination of kinase and phosphatase activities. A myosin phosphatase inhibitor protein CPI-17 is phosphorylated at Thr38 through G-protein-mediated signals, resulting in a >1000-fold increase in inhibitory potency. We show here the solution NMR structure of phospho-T38-CPI-17 with rmsd of 0.36 ± 0.06 Å for the backbone secondary structure, which reveals how phosphorylation triggers a conformational change and exposes an inhibitory surface. This active conformation is stabilized by the formation of a hydrophobic core of intercalated side chains, which is not formed in a phospho-mimetic D38 form of CPI-17. Thus, the profound increase in potency of CPI-17 arises from phosphorylation, conformational change, and hydrophobic stabilization of a rigid structure that poses the phosphorylated residue on the protein surface and restricts its hydrolysis by myosin phosphatase. Our results provide structural insights into transduction of kinase signals by PP1 inhibitor proteins.

INTRODUCTION

Type-1 Ser/Thr phosphatase (PP1) is conserved among all eukaryotes and is responsible for regulation of a plethora of cellular functions. A specific multisubunit form of PP1, called myosin phosphatase, is a ubiquitous enzyme that functions in various signaling circuits (Hartshorne et al., 2004). Myosin phosphatase consists of a catalytic subunit of PP1 and a myosin targeting MYPT1 subunit with an accessory M21 subunit (Hartshorne et al., 2004). The N-terminal ankyrin-repeat domain of MYPT1, including a PP1 binding site, functions as an allosteric regulator of the catalytic subunit (Terrak et al., 2004). On the other hand, the C-terminal domain is phosphorylated by multiple kinases, ROCK, ZIPK, and ILK, resulting in the inhibition of myosin phosphatase (Trinkle-Mulcahy et al., 1995; Kimura et al., 1996; MacDonald et al., 2001; Muranyi et al., 2002). In smooth muscle, agonist-induced activation of G protein enhances the activity of Ca^{2+}/calmodulin-dependent myosin light-chain kinase and coincidently suppresses the activity of myosin phosphatase via the activation of kinases ROCK and PKC (Kitazawa et al., 1991; Somlyo and Somlyo, 2003). The inhibition of myosin phosphatase is required for robust and sustained contraction of smooth muscle in response to agonist stimuli (Dimopoulos et al., 2007), as well as regulation of cytoskeletal reorganization during cell migration (Kawano et al., 1999) and cytokinesis (Matsumura, 2005).

In addition to direct phosphorylation of the MYPT1 subunit, myosin phosphatase is regulated by a specific inhibitor protein, CPI-17, that is predominantly expressed in smooth muscles and neurons (Eto et al., 1997, 2002a; Woodsome et al., 2001). Phosphorylation of CPI-17 at Thr38 is necessary and sufficient to convert the protein into a potent inhibitor of myosin phosphatase (Eto et al., 1995; Kitazawa et al., 2000; Koyama et al., 2000; Pang et al., 2005). By contrast, other multisubunit forms of PP1 in cells are insensitive to phospho-CPI-17 (P-CPI-17) (Senba et al., 1999). One example is a glycogen-bound form of PP1 holoenzyme, which binds P-T38-CPI-17 but dephosphorylates it (Eto et al., 2004). With myosin phosphatase, there is binding of P-T38-CPI-17, but the hydrolysis step is arrested, resulting in formation of inactive complex. Thus, P-T38-CPI-17 can be a substrate or an inhibitor of different forms of PP1, depending on regulatory subunits (Eto et al., 2004).

In smooth-muscle cells, rapid phosphorylation of CPI-17 at Thr38 occurs in parallel to phosphorylation of myosin

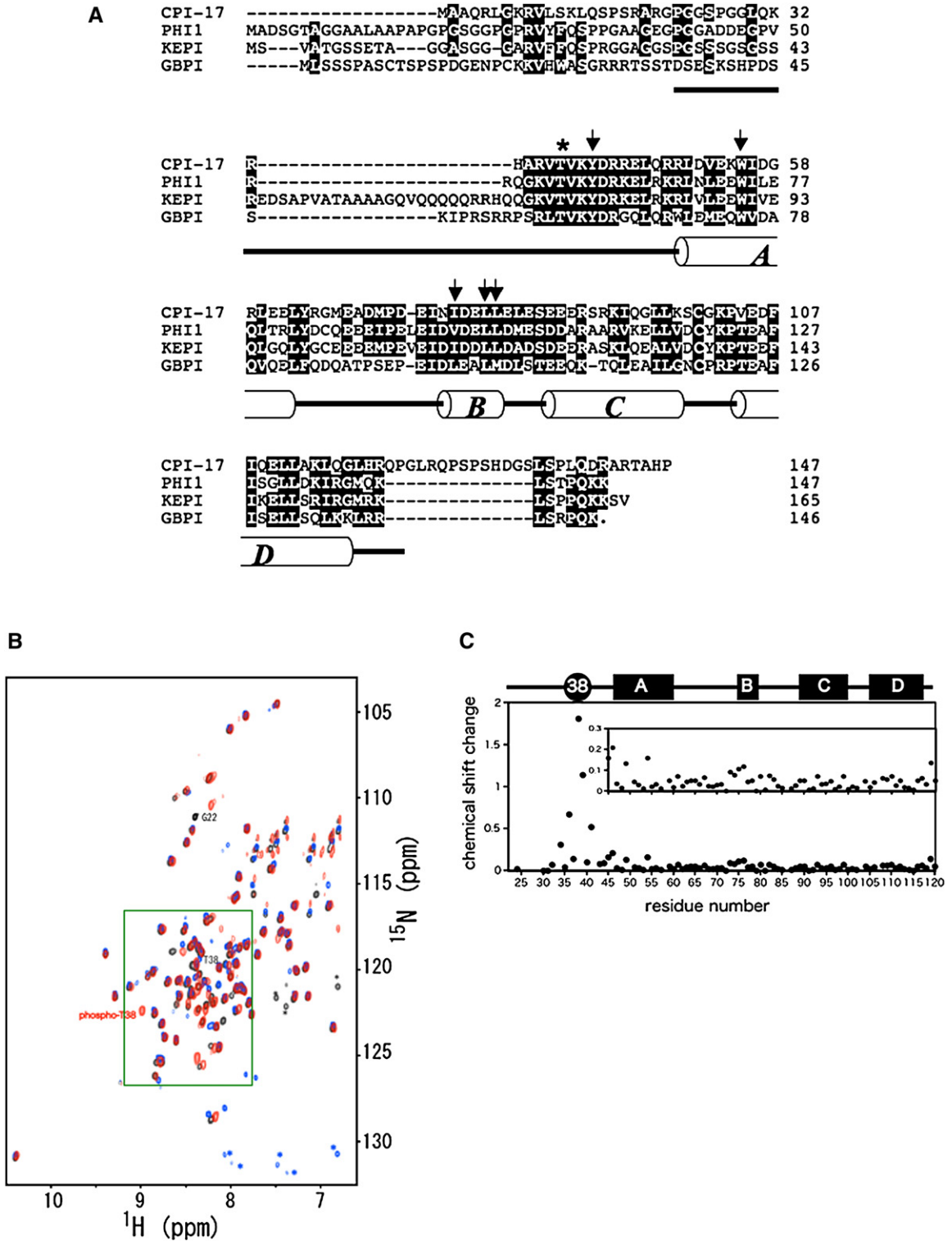

Figure 1. Inhibitory Domain of CPI-17 Family

(A) Amino acid sequence of CPI-17 family of PP1 inhibitor proteins. Asterisk indicates Thr38, and arrows indicate Trp55, Ile77, Leu80, and Leu81. Cylinders show regions in helices A to D.

(B) ^{1}H-^{15}N HSQC spectrum. ^{15}N single labeled P- (red), U- (gray), and D38-CPI-17 (22–120) (blue) were subjected to HSQC measurement at 1 mM protein concentration. All amide resonances were assigned to each residue (data not shown). Box line indicates the area shown in Figure S2. Asterisk indicates fold-back peak of resonance derived from side-chain amide.

via activation of Ca^{2+}-dependent PKC, followed by prolonged phosphorylation, maintained via RhoA/ROCK signal (Dimopoulos et al., 2007). Phosphorylation of CPI-17 is reduced through a cGMP-dependent pathway in response to nitric oxide release, in parallel to muscle relaxation (Bonnevier and Arner, 2004; Etter et al., 2001). Thus, in smooth muscles CPI-17 functions to mediate multiple signals into myosin phosphatase and thereby control myosin phosphorylation and contraction. Fluctuation in the expression and the phosphorylation levels of CPI-17 is associated with smooth-muscle-related diseases, such as intestinal bowel disease (Ohama et al., 2003), asthma (Sakai et al., 2005), pulmonary hypertension (Dakshinamurti et al., 2005), and diabetic dysfunction of smooth muscle (Chang et al., 2006; Xie et al., 2006). In Purkinje neurons, CPI-17 is essential to maintain G-protein-mediated AMPA receptor internalization and generate long-term synaptic depression in response to stimulation (Eto et al., 2002a). In addition, the upregulation of CPI-17 was found in tumor cells, which causes hyperphosphorylation of tumor suppressor merlin (NF2) and transformation of cells (Jin et al., 2006). Therefore, CPI-17 poses a potential target of pharmaceutical approaches for these diseases.

Determination of the three-dimensional (3D) structure of unphospho-CPI-17 by NMR revealed a 2 × 2 pairing of a four-helix bundle, forming a unique V-shape structure (Ohki et al., 2001). The phosphorylation site, Thr38, is located in a loop structure (P loop) at the N terminus, sitting in a cavity between helices (Ohki et al., 2001). When Thr38 is substituted for Asp to mimic phosphorylation, the P loop becomes exposed to solvent, suggesting a conformational change of the P loop upon activation of CPI-17 (Ohki et al., 2003). However, structural analysis of the basis for enhanced inhibition of myosin phosphatase by CPI-17 was limited because the D38-form of CPI-17 is significantly less potent, compared with phospho (P)-T38-CPI-17 (Ohki et al., 2003). We concluded that despite a conformational change in the D38 protein, this structure was not the same as that of the highly potent and fully activated P-T38-CPI-17. Therefore, we prepared CPI-17 protein fully phosphorylated with PKC and determined the 3D structure by using multidimensional NMR techniques. The 3D structure indicates a global conformational switch upon phosphorylation of CPI-17 at Thr38, shows differences relative to the phospho-mimetic D38 structure, and exposes novel interactions between P-CPI-17 and myosin phosphatase.

RESULTS

Phosphorylation of CPI-17

The inhibitory domain of CPI-17 comprised of residues 22–120 is conserved among the CPI-17 family of PP1 inhibitor proteins, such as PHI-1, KEPI, and GBPI (Figure 1A). The recombinant $^{13}C/^{15}N$-labeled 22–120 protein was phosphorylated to completion by extended incubation with purified PKC (Figure S1, see the Supplemental Data available with this article online) and subjected to a series of multidimensional NMR experiments (Figure 1B and Figures S2 and S3). Figure 1B shows the ^{1}H-^{15}N HSQC spectrum of $^{13}C/^{15}N$-labeled P-CPI-17 (red) superimposed on the previous spectra of unphosphorylated (gray) and Asp-substituted D38-CPI-17 (blue) (22–120) proteins (Ohki et al., 2003). Overall, the profiles of HSQC spectra in the full-scale chart are similar in all three forms of CPI-17 examined by NMR (Figure 1B). The backbone amide resonance of Thr38 is shifted to downfield upon phosphorylation (Figure 1B and Figure S2). This phosphorylation-dependent downfield shift is consistent with a previous report on phosphorylation of the tau protein (Landrieu et al., 2006). Concomitantly, a large chemical shift change of amide resonances from the neighbor residues was observed in the phosphorylation loop (P loop), such as V39 and Y41 (Figure 1C). In addition, clusters of moderate changes in chemical shift were observed from residues around A helix (residue 44–46) and B helix (residue 74–83) (Figure 1C, inset). The chemical shifts of these residues in P-T38-CPI-17 did not match those in the D38 form of CPI-17 (Figure 1B and Figure S2, blue). This suggests that the conformation of the phosphorylated protein differs from the conformation of the protein with a ''phosphomimetic'' mutation to introduce an Asp at the same residue. There was no evidence of multiple conformation states in the spectrum of P-T38-CPI-17.

Structure of Phospho-T38-CPI-17

The 3D structure of P-T38-CPI-17 was calculated with 1,518 structural restraints obtained from the NMR data (Figure S3), summarized in Table S1. Overall, the topology of P-T38-CPI-17 is composed of a long loop with the phosphorylation site, Thr38, followed by a left-handed four-helix bundle (termed A to D from the N terminus) (Figure 2). The four helices are arranged in an antiparallel orientation. The structure of residues 22 to 31 at the N terminus of the truncated protein was in a flexible conformation, seen by lack of long-range NOE. This conclusion is supported by very small heteronuclear ^{15}N-$\{^{1}H\}$ NOE values (Figure S4) and the fast H-D exchange rates (data not shown) of these ten residues. In contrast, the conserved region of residues 32 to 40 with phospho-Thr38 (P-Thr38), termed the P loop, converged into a single conformation with a backbone rmsd of 1.18 ± 0.27 Å, with relatively higher heteronuclear ^{15}N-$\{^{1}H\}$ NOE values (Figure S4, red). The P-Thr38 side chain is exposed to solvent, and the P loop lays on the surface of the four-helix bundle. The side chains of Val37 and Val39 face into the protein, making contacts with Ile56 and Tyr41/Val52/Ile77, respectively. These two Val residues function to

(C) Chemical shift change of amide resonance induced by phosphorylation at Thr38. The chemical shift change was calculated as described in Experimental Procedures and plotted against residue numbers. Regions of the phosphorylation site and α helices are indicated above as a circle and boxes, respectively.

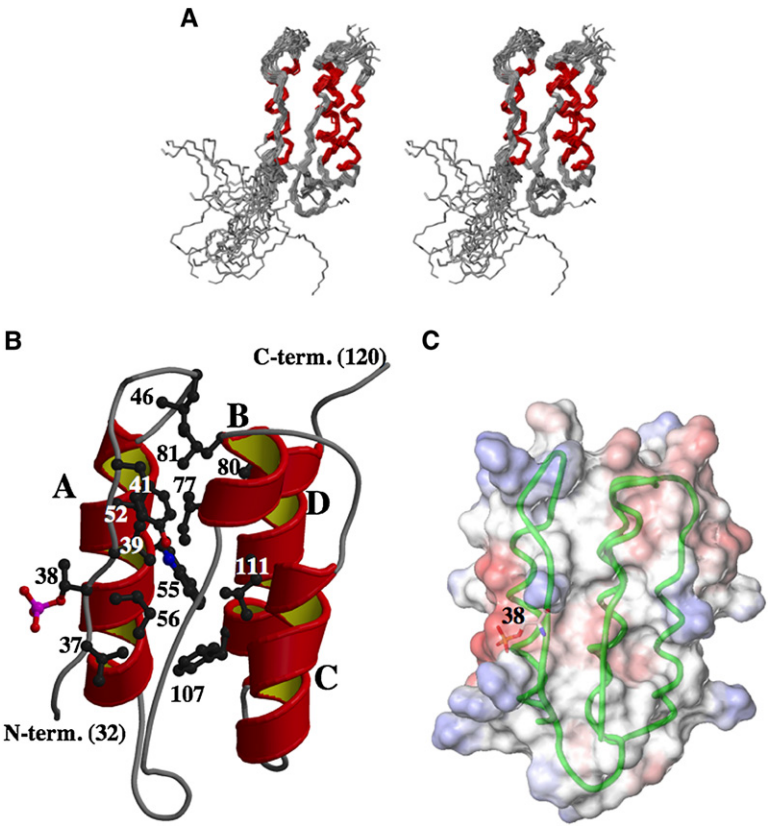

Figure 2. Solution NMR Structure of Phospho-CPI-17(22–120)

(A) Stereo view of the backbone of 20 superimposed structures obtained by NMR analysis. Red indicates the region of α helix.

(B) Ribbon representation of an energy-minimized average structure. In the ribbon model, the flexible N-terminal 31 residues are not depicted. T38 and residues involved in hydrophobic clustering are drawn with ball-and-stick side chains labeled with residue numbers to facilitate identification, and the helices are labeled with upper case letters.

(C) Space-filling representation with molecular surface potential, superimposed on backbone structure (green). Red and blue on surface indicate regions of negative and positive charges, respectively. A side chain of P-T38 is drawn as ball and stick.

anchor the P loop to the four-helix bundle by hydrophobic interactions of the aliphatic side chains.

Comparison between Unphospho-, Phospho-, and Asp-Substituted CPI-17 Structures

Comparison of P-T38-CPI-17 structure with that of the unphospho-form (U-CPI-17) and D38-form (Ohki et al., 2003) reveals global conformational change in response to phosphorylation (Figure 3) (Table S2). The most remarkable difference is the position of the key residue, Thr38, whose side chain comes out of a cavity between A and B helices upon phosphorylation. When structures are superimposed with the A/D helix pair for alignment (Figure 3, bottom), the phosphorylation at Thr38 is seen to trigger a swinging motion of the P loop around the A helix, resulting in 8.1 Å movement of residue 38. The swing of the P loop is coupled with a right-handed rotation of A helix by 29 degrees, along with a complementary rotation of the D helix. These rotations expose new surfaces of both helices that become available for binding to myosin phosphatase. Similar to U-CPI-17, the A/D helix pair in P-T38-CPI-17 is stabilized by hydrophobic residues as shown in Figure 3. In concert with motion of the A helix, the B/C helix pair becomes close to the A/D helix pair. This aligns the four helices into an antiparallel bundle (Table S3). The average distance between the four helices becomes 15% shorter (Table S3), and the compaction of the structure causes the overall surface area of the protein to be reduced from 7,221 to 6,374 Å^2. Substitution of T38 to Asp results in the P loop becoming exposed to solvent, consistent with changes in P form. However, the realignment of four helices is not evident in the D38 protein relative to the U-CPI-17, and the overall structure remains V shape (Figure 3, center).

Formation of Hydrophobic Core

The phosphorylation-induced compression of the four helices gathers Tyr41 in the P loop, Leu46/Val52 in A helix, and Ile77/Leu80/Leu81 in B helix into a stable hydrophobic core (Figure 4A). For example, the distance between Val 52 and Ile77 Cα atoms shortens from 19.0 to 6.4 Å. Such hydrophobic clustering likely causes changes in chemical shift of residues around A and B helices (Figure 1C) and functions to stabilize the antiparallel-aligned four-helix bundle of P-CPI-17. This stabilization reflects in higher heteronuclear NOE value of P-T38-CPI-17, compared with U- and D38-CPI-17 (Figure S3). We assayed thermal stabilities of U- and P-T38-CPI-17, and indeed, phosphorylation increased the mean melting temperature T_m from 59°C (U-CPI-17) to 64°C (P-T38-CPI-17), showing an effect on the thermodynamic stability of the protein. We attribute this change to the hydrophobic core in P-T38-CPI-17 (Figure 4B). The hydrophobic core is not well defined in the D38-CPI-17 structure (Figure 4A, middle). Consistent with this observation, we found the thermal stability of D38-CPI-17 was lower (T_m = 54°C), compared to P-T38-CPI-17 (Figure 4B). Overall, the structure and thermal stability are consistent with the idea that

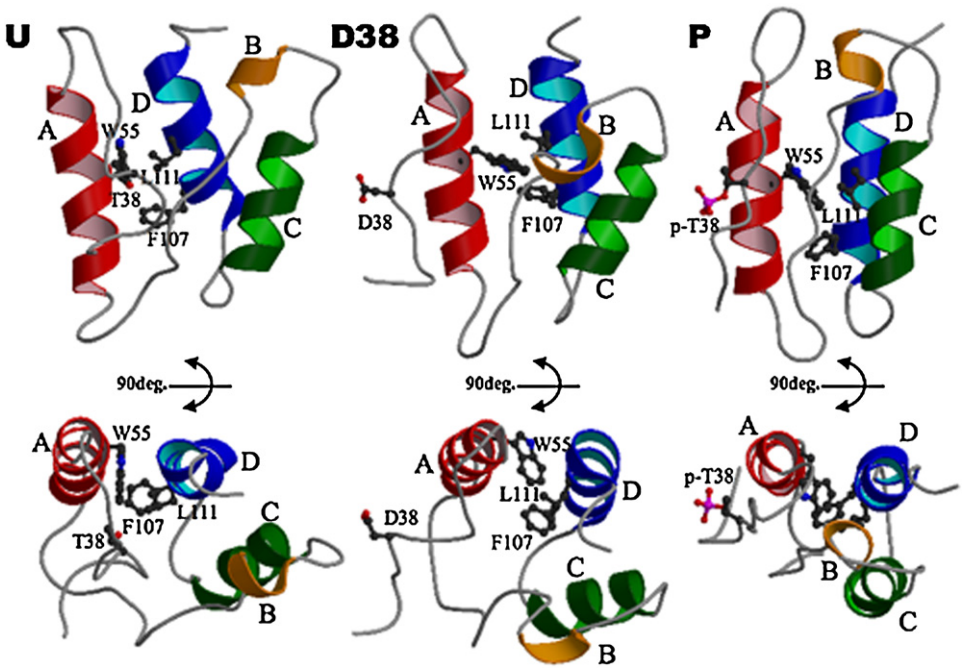

Figure 3. Conformational Transition of CPI-17 upon Phosphorylation
U-CPI-17 (1J2M) (left), D38-CPI-17 (1J2N) (middle), and P-T38-CPI-17 (right) are displayed as ribbon structures. Side chains of hydrophobic residues that tether helix A to D are shown as ball and stick for emphasis.

phosphorylation but not mutation to an acidic residue triggers condensation of the protein into a rigid structure, with a surface topography distinctly different from the unphosphorylated protein.

The Hydrophobic Core of P-T38-CPI-17

We examined effects of mutation of residues in the hydrophobic core on the inhibition of purified myosin phosphatase with wild-type CPI-17 and Y41A, W55A, D73A/E74A, and I77A/L80A/L81A mutants. All these recombinant CPI-17 were equally phosphorylated by purified PKC, suggesting that the mutations do not impair reaction with Thr38 (Table S4). However, the phosphorylated mutant CPI-17 showed different inhibitory potency (Figure 5A). Mutation at either Trp55 or Asp73/Glu74 caused moderate reduction in inhibitory potency, and the triple mutation of Ile77/Leu80/Leu81 showed greatly reduced potency, to an IC_{50} of around 100 nM. Our previous data showed that an Ala mutation at Tyr41 (Y41A) eliminated the inhibitory activity of CPI-17 (Hayashi et al., 2001). Thermal stability of the Y41A protein (T_m = 56°C) was lower than that of wild-type (Figure 4B, cross). We concluded that the hydrophobic clustering of Y41 and Ile77/Leu80/Leu81 was required for potency of CPI-17 as an inhibitor for myosin phosphatase. The function of CPI-17 mutated in the hydrophobic core was examined with beta-escin-permeabilized vas deferens smooth-muscle tissues (Figure 5B). Because CPI-17 is present at only negligible levels in vas deferens smooth muscle, phorbol ester (PDBu, a PKC activator) stimulation does not induce force production at limiting Ca^{2+} concentrations (Figure 5B, arrowhead) (Woodsome et al., 2001). Doping of recombinant U-CPI-17 into a permeabilized vas deferens smooth-muscle strip restored PDBu-induced force production at clamped Ca^{2+} concentration, suggesting that PKC induced the phosphorylation of CPI-17 causing inhibition of the endogenous myosin phosphatase in the strip (Figure 5B, double arrowhead). The triple mutant CPI-17, I77A/L80A/L81A or Y41A (Figure 5B), did not induce PKC-mediated smooth-muscle contraction, suggesting that the formation of hydrophobic core is necessary for CPI-17 to inhibit myosin phosphatase in tissues. On the other hand, CPI-17 mutants D73A/E74A and W55A supported PDBu-induced force production. The maximum extent and the rate of force development were slightly lower with these mutant proteins, compared with wild-type. We note that D73, E74, and W55 are conserved among CPI-17 proteins from various species, so changes in these residues have not survived probably because of the changes in properties.

Modeling of the Interaction between P-T38-CPI-17 and Myosin Phosphatase

The phospho-pivot computer modeling method was used to examine hypothetical docking of P-T38-CPI-17 with myosin phosphatase (Eto et al., 2004; Matsuzawa et al., 2005a, 2005b). The phosphate group of P-T38-CPI-17 was set into the active site of PP1δ•MYPT1(1–299) complex (Terrak et al., 2004), and 186,624 in silico complexes were generated by rotating P-T38-CPI-17 around the phosphorus atom as a pivot. Each model complex was scored based on only atomic distances between two

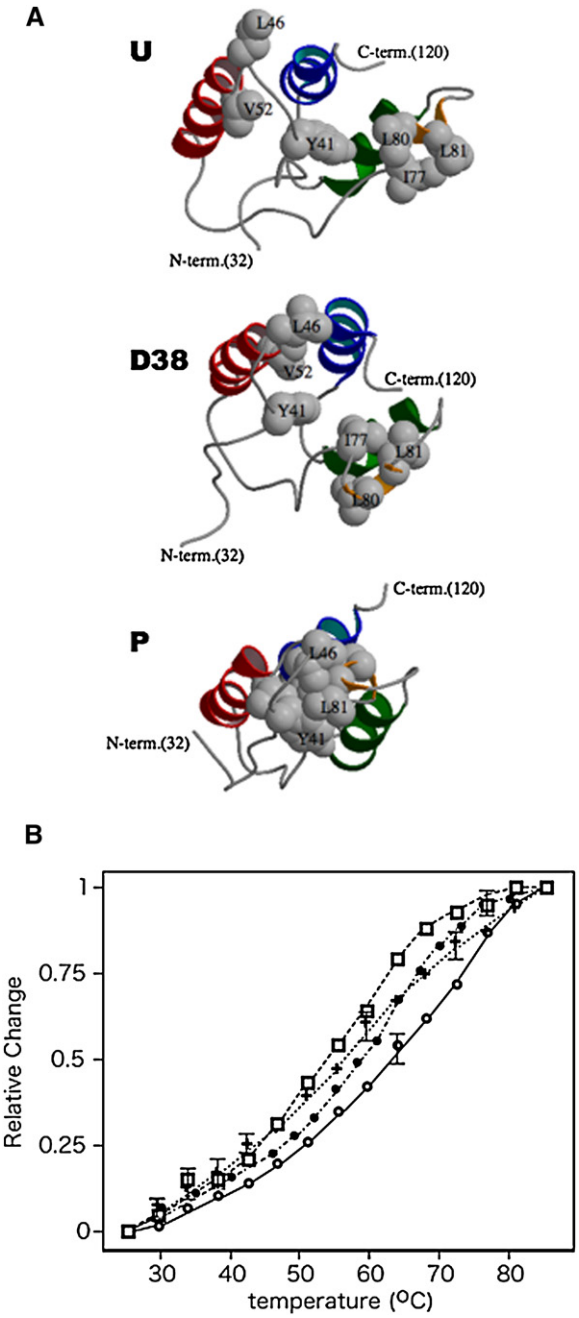

Figure 4. Formation of the Hydrophobic Core in P-CPI-17

(A) Top, middle, and bottom panels represent the structures of U-, D38-, and P-T38-CPI-17, respectively. Hydrophobic side chains responsible for the condensed conformation are displayed as Corey, Pauling, and Koltun colored model.

(B) Thermal stability of CPI-17 proteins monitored by circular dichroism (CD). Vertical axis shows relative change of the molar ellipticity at 222 nm at indicated temperature. CD spectrum was measured with 20 μM protein; P-T38-CPI-17 (open circle), U-CPI-17 (closed circle), D38-CPI-17 (rectangle), and P-T38-CPI-17 (Y41A) (cross), in 50 mM potassium phosphate buffer (pH 7.0). Mean values from triplicate assays are shown. Error bars indicate SEM values from three independent assays.

proteins. The modeling yields one converged structure of P-CPI-17 on myosin phosphatase (Figure 6A). In this complex, the P loop fits in the active site groove of PP1, from the cavity of ankyrin-repeat domain toward the N-terminal α-helical segment of MYPT1 (Terrak et al., 2004). This model suggests that four Arg side chains in P loop, Arg33, Arg36, Arg43, and Arg44, are involved in the interaction with myosin phosphatase, in addition to phospho-Thr38. This is consistent to our previous results that an Ala mutation of CPI-17 at Arg43 and Arg44 impairs the inhibitory potency over 40-fold (Hayashi et al., 2001). Interestingly, this model positions N-terminal α-helical segment of MYPT1 in close proximity to P-T38-CPI-17 (Figure 6A).

Binding of P-T38-CPI-17 to MYPT1

Experimental testing of this model with immobilized peptides corresponding to MYPT1 segments (1–19) and (24–41) showed binding of P-T38-CPI-17 to MYPT1(1–19), but not to MYPT1(24–41) (Figure 6B). Furthermore, we examined the role of MYPT1 N-terminal segment by pull-down assay with recombinant myosin phosphatase complex (Figure 6C). Myosin phosphatase complexes, consisting of myc-tagged MYPT1(1–300) or MYPT1(18–300) with HA-tagged PP1 delta were generated in HEK293 cells by transient transfection, as described previously (Eto et al., 2005). The cotransfection method produces active form of myosin phosphatase complex in cells (Eto et al., 2005). Approximately equivalent amounts of myc-MYPT1 were detected in the lysates by immunoblotting with anti-myc antibody (Figure 6C, left). However, the binding of myc-MYPT1(18–300) to thioP-CPI-17 beads was ten times weaker, compared with (1–300) (Figure 6C, left). Taken together, these data show the N-terminal α-helical segment of MYPT1 in myosin phosphatase complex contributes to the interaction with P-CPI-17.

DISCUSSION

From comparison of the structures of the inactive U-CPI-17 and the active P-T38-CPI-17, we identify a conformational transition upon phosphorylation of CPI-17 at Thr38. The phosphorylation induces a swing of the P loop and a formation of the hydrophobic core to lock and stabilize a condensed active conformation of P-T38-CPI-17. Compared with residues in P loop and Leu46, changes in chemical shift of I77/L80/81 were relatively small. Presumably, interactions with side chains of Y41 and L46 give a minimum effect on the hydrophobic environment in the cluster of I77/L80/81, which is evident in the unphospho form. Nonetheless, an environmental change around B helix is detected as a cluster of chemical shift changes. Besides, Ala-substitution mutants clearly demonstrate a major contribution of hydrophobic side chains of I77/L80/81 to the inhibitory potency. Therefore, we conclude that this swing-and-lock mechanism of CPI-17 is responsible for potent and specific inhibition of myosin phosphatase to switch phosphorylation levels of myosin and merlin in response to G-protein activation. All PP1-specific inhibitor proteins are regulated by phosphorylation, and five of

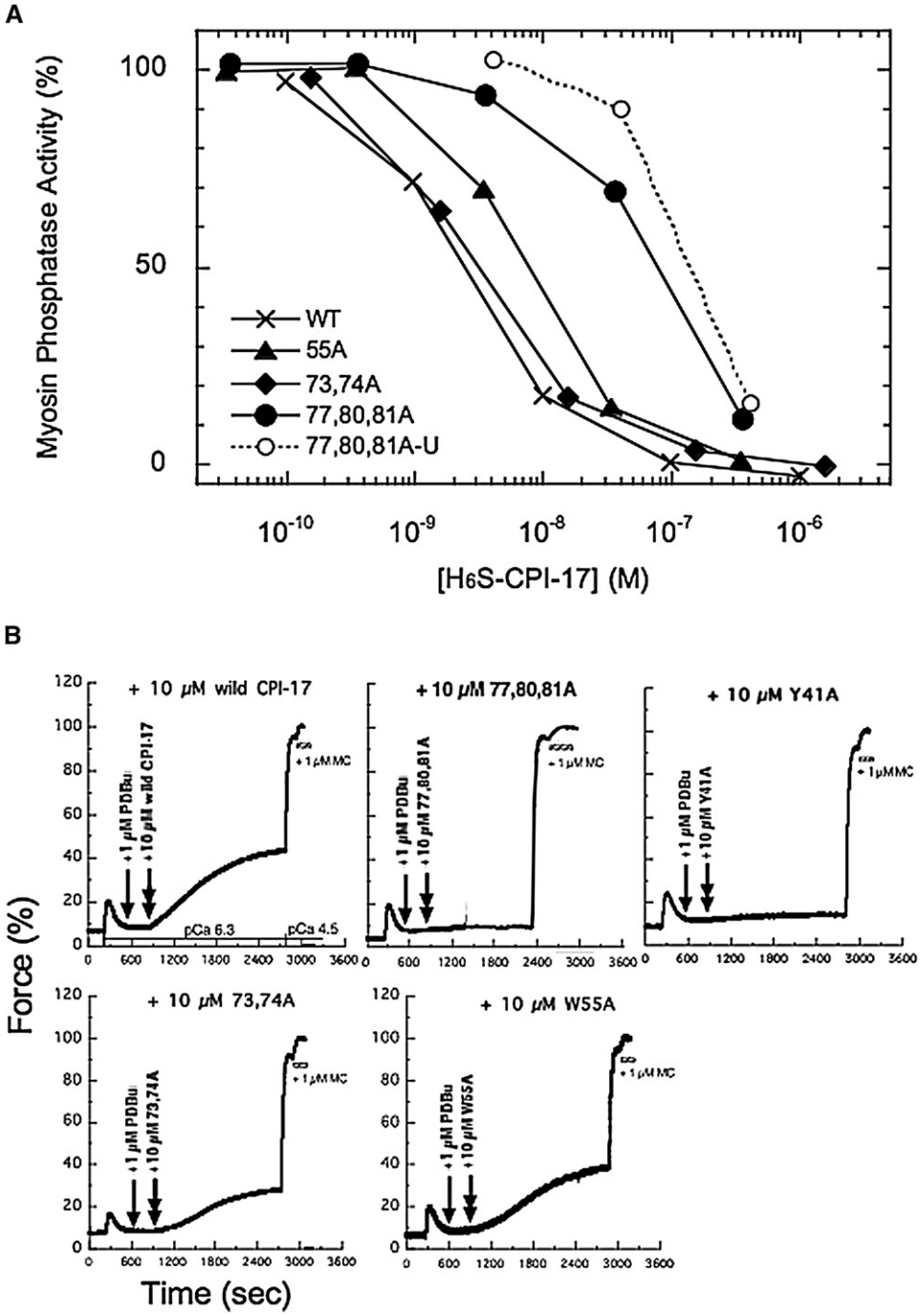

Figure 5. Effects of the Mutation in the Hydrophobic Core on the Inhibitory Potency of CPI-17

(A) Inhibition of myosin phosphatase purified from pig aorta. The myosin phosphatase activity without inhibitor proteins was set as 100%. Data are averaged from two independent assays done in duplicate.

(B) Force measurement of vas deferens smooth-muscle strip. Panels represent the time-dependent force trace with U-CPI-17: wild-type, D73A/E74A, I77A/L80A/L81A, and W55A. The rabbit vas deferens smooth-muscle strips were permeabilized with beta-escin. The CPI-17 proteins were doped into the tissue after the addition of PDBu. The extent of contraction in the presence of 1 μM Ca^{2+} is set as 100% value.

them are in the CPI-17 family, based on the similarity of the sequences including residues in the hydrophobic core identified here by NMR, so these results should apply to other CPI-17 family members. On the other hand, phosphorylation of another class of PP1 inhibitors, inhibitor-1 and DARPP-32, apparently only induces a minor conformational change in the molecule, despite over 1,000-fold increase in the inhibitory potency (Endo et al., 1996;

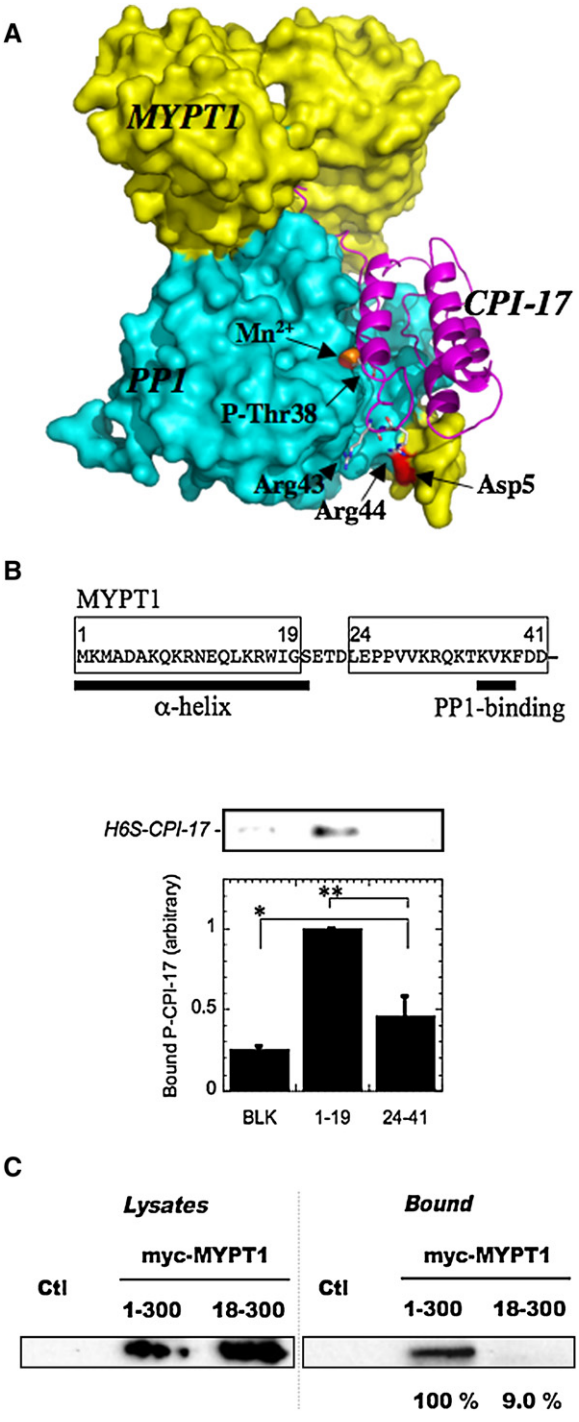

Figure 6. Interaction of P-CPI-17 with PP1•MYPT1 Complex

(A) Hypothetical 3D model of MYPT1(1–299)•PP1•P-CPI-17 complex. The coordinates of MYPT1(1–299)•PP1 complex (PDB code: 1S70) were used for computer modeling of the complex. MYPT1 (yellow) and PP1 (cyan) are depicted in a surface model, and P-T38-CPI-17 is drawn as a ribbon structure. The positive charge of MYPT1 Asp5 is shown as red, and the side chains of phospho-Thr38 and Arg43/44 in CPI-17 are shown as ball-and-stick.

(B) Direct binding of P-CPI-17 with MYPT1(1–19) peptide. Binding assay of P-T38-CPI-17 was performed with synthetic peptides corresponding to MYPT1 segments (1–19) and (24–41), immobilized on agarose beads. Bound P-T38-CPI-17 was quantified by immunoblotting with anti-CPI-17 antibody (top). Normalized values are represented as a bar graph. Student's t test was used to assess significance, and asterisk and double asterisk indicate $p > 0.15$ and $p < 0.03$, respectively. Error bars indicate SEM values from three independent assays.

(C) Pull-down assay of myc-MYPT1•PP1 complex and P-CPI-17. Recombinant myc-MYPT1(1–300) and myc- MYPT1(18–300) were transiently expressed in HEK293 cells, and the crude lysates were used as a source of recombinant myosin phosphatase complex. Panels demonstrate immunoblots with anti-myc antibody for myc-MYPT1 in cell lysates (left) and in the fraction bound to thiophospho-CPI-17 beads (right). Bound myc-MYPT1 was normalized against that in cell lysate, and mean values from two independent experiments are represented under each lane.

Neyroz et al., 1993). The phosphorylation-induced conformational switch seems to be a unique feature in the CPI-17 family of PPI inhibitor proteins.

Asp- or Glu-substitution of Ser or Thr is often used for mimicking phosphorylation of proteins. One example is the activation loop of protein kinases. Phosphorylation of protein kinases in the activation loop is required for full activity, and it can be mimicked by substitution with Asp or Glu (Zhang et al., 1995). The phosphate group in the activation loop of kinases directly forms salt bridges with Arg residues in N-terminal domain (Canagarajah et al., 1997; Johnson et al., 1996), and the effectiveness of Glu or Asp suggests these residues can form salt bridges with the same Arg. In contrast, the phosphate of P-T38-CPI-17 is exposed to solvent and interacts instead with the active site of PP1 in myosin phosphatase. Asp substitution at Thr38 induces a swing of the P loop but not the same realignment of helices or formation of the hydrophobic core in the protein as is formed when T38 is phosphorylated (Ohki et al., 2003). The failure of hydrophobic clustering in D38-CPI-17 is evidenced by lower thermal stability. Without the hydrophobic core there is a 100-fold lower inhibitory potency of D38-CPI-17 compared to P-T38-CPI-17. Thus, the negative charge of a carboxyl group is insufficient for completion of the conformational switching in CPI-17. This gives an example of where an acidic side chain is not phosphomimetic, offering a note of caution to the common practice of using properties of mutated proteins to make conclusions about effects of phosphorylation.

Currently, about 150 protein structures with phospho-Thr are listed in the Protein Data Bank (PDB). In most cases, the phosphate group is directly tethered to other residues in the same protein via salt bridges and/or hydrogen bonds. In this way, the phosphate drives formation of a new protein conformation that is stabilized by these intramolecular interactions, as seen in glycogen phosphorylase-a and protein kinases (Johnson et al., 1996; Sprang et al., 1988). Another example is the NMR structure of a 44 residue P-Thr peptide mimicking the forkhead-associated (FHA) domain of human Ki67 protein in the complex with its receptor, the human nucleolar protein hNIHK, where the phosphate functions as a ligand (Byeon et al., 2005). Our studies reveal a different mechanism of phosphorylation-induced conformational change. The phospho

conformation of the CPI-17 P loop is stabilized without a hydrogen bond or salt bridge to the phosphate group from other residues in the protein. Based on heteronuclear NOE data, the P loop of unphosphorylated CPI-17 is highly flexible, and this presumably exposes Thr38 to kinases, such as PKC and ROCK. Upon the phosphorylation of T38, the side chains of neighboring V37, V39, and Y41 anchor the P loop to the hydrophobic core formed between the helices that restrains the overall solution structure. The rigid structure of phosphorylated P loop is likely critical for the potent inhibition of the phosphatase by positioning the phosphate relative to other residues in CPI-17 that form contacts with MYPT1 and PP1. When the hydrophobic core of P-T38-CPI-17 is perturbed by Ala substitution of Tyr41, the P-Thr38 residue is readily dephosphorylated by myosin phosphatase (Hayashi et al., 2001). We propose that the rigidity of the structure due to the hydrophobic core is key to preventing hydrolysis of the P-T38, making P-T38-CPI-17 an inhibitor instead of a substrate. Thus, the swing-and-lock mechanism of CPI-17 activation restricts flexibility of the P loop and protects P-Thr38 from being hydrolyzed at the active site of myosin phosphatase. Interestingly, P-T38 is hydrolyzed by other PP1 holoenzymes, such as glycogen phosphatase (a heterodimer of PP1 plus GM subunit; Eto et al., 2004), so phospho-CPI-17 is both a substrate and an inhibitor, depending on the form of PP1 it encounters.

Previously, phospho-pivot modeling with D38-CPI-17 (PDB code: 1J2N) and monomeric PP1 alpha isoform catalytic subunit (PDB code: 1IT6) predicted critical roles for residues at the active site of PP1δ, namely D137, D193, R220, Y271, and E274. Indeed, these residues are necessary for the binding of PP1 δ with P-T38-CPI-17 in an in vitro assay (Matsuzawa et al., 2005a). These same residues at the PP1 active site seem to be involved in the model of the P-T38-CPI-17•PP1δ•MYPT1(1–299) complex. However, the best fitting model was obtained when the pivot phosphorus atom was set at a position 0.5 Å away from the active site. Thus, the phosphate group is not in an optimum position for hydrolysis in this model. We speculate that weak interactions of the MYPT1 subunit with P-T38-CPI-17, perhaps involving Asp5 of MYPT1 N-terminal segment and Arg44 of P-CPI-17 (Figure 6A), displaces phospho-Thr38 from being in an optimum position at the PP1 active site for dephosphorylation. Some involvement of MYPT1 seems to be needed to account for the inhibitor versus substrate reaction of P-T38-CPI-17 with different PP1 holoenzymes.

It is noteworthy that the phospho-pivot model positions the unstructured N-terminal tail of CPI-17 near the MYPT1 ankyrin repeat domain. Other CPI-17 family members, PHI-1 and KEPI, also inhibit myosin phosphatase, but with different potencies. The IC_{50} for PHI-1 (50 nM) is 50-fold higher than that for CPI-17, whereas KEPI inhibits myosin phosphatase with IC_{50} of 0.1 nM (Erdodi et al., 2003; Eto et al., 1999). It is possible that the N-terminal tail of the different CPI-17 family members functions as a sensor for different regulatory subunits of PP1. This gives us a future direction for studying functional diversity in the CPI-17 family. Despite a focus on the MYPT1 N-terminal domain, we cannot completely rule out involvement of the MYPT1 C-terminal domain and/or the M21 subunit in specific recognition of P-CPI-17. Other PP1 inhibitor proteins are known to contact both PP1 catalytic and regulatory subunits to form trimeric complexes that account for their selective inhibition of PP1 in different contexts. One example is inhibitor-1 binding to GADD-34 that is bound to PP1, and other examples are inhibitor-2 binding to either neurabin or KPI-2 that both bind PP1 at independent sites. (Connor et al., 2001; Terry-Lorenzo et al., 2002; Wang and Brautigan, 2002). PP1 inhibitor proteins also bind to PP1 holoenzymes without direct contact to regulatory subunits, such as heterotrimers of inhibitor-2 with Nek2A•PP1 (Eto et al., 2002b; Li et al., 2007) and inhibitor-3 with sds22•PP1 (Lesage et al., 2007). Direct contact between regulatory subunits and PP1 inhibitor proteins is an attractive idea to provide signaling specificity for controlling individual PP1 complexes. The structure of an activated PP1 inhibitor gives general insight into phosphorylation-dependent conformational changes and regulation of cellular PP1, and opens a door to understanding mechanisms of signaling crosstalk between kinases and phosphatases.

EXPERIMENTAL PROCEDURES

Proteins

The cDNA of CPI-17 was cloned from pig aorta smooth muscle library. Recombinant CPI-17(22–120) for NMR was prepared with pET30 bacterial expression vector with the minimal medium containing ^{15}N-ammonium chloride and/or ^{13}C-glucose as the sole source of nitrogen and/or carbon. This method yields the uniformly stable-isotope-labeled (>95%) sample for NMR spectroscopy (Ohki et al., 2001, 2003). CPI-17 proteins for other assays are expressed as full-length versions with N-terminal His_6- and S-tag sequences (Eto et al., 2003). Phosphorylation of the protein was performed with an active fragment of PKC. The active fragment of PKC was extracted from human red cells with hypotonic buffer and purified by ammonium-sulfate precipitation and sequential column chromatography with DEAE-Sepharose, Phenyl-Sepharose, Q-Sepharose, and Protamine-agarose. Stoichiometric phosphorylation of CPI-17 was verified by urea-PAGE analysis (Figure S1), as described previously (Eto et al., 2003). Anti-P-T38-CPI-17 IgY was prepared by using synthetic phospho-peptide as an antigen (Aves Lab, Tigard, OR) and purified by affinity chromatography, as described previously (Kitazawa et al., 2000).

NMR Structure Determination

All NMR data for ~1 mM P-T38-CPI-17 (in 50 mM phosphate buffer [pH 6.8], 100 mM KCl, 1 mM DTT, and 0.02% NaN_3) were recorded on a Varian INOVA750 spectrometer. The sample temperature was kept at 25.0°C. A set of two- and three-dimensional NMR data was obtained for resonance assignments (Bax and Pochapsky, 1992). Homonuclear 2D-NOESY, ^{15}N-edited NOESY, and ^{13}C-edited NOESY with mixing time of 100 ms were recorded to collect distance information. To obtain the information about hydrogen bonding, amide proton H-D exchange was monitored by ^{1}H-^{15}N HSQC. 2D-HMQC-J spectra were also recorded to obtain dihedral angle constraints. All NMR data were processed with nmrPipe/nmrDraw (Delaglio et al., 1995) and were analyzed with PIPP (Garrett et al., 1991). Structure calculation was carried out with X-PLOR version 3.851 (Brunger et al., 1998; Kleywegt and Jones, 1998). Quality of each coordinate was examined by using AQUA/procheck-NMR (Laskowski et al., 1996). The Ramachandran plot analysis of the final structures showed that 1.7 ± 1.1% of

nonglycine and nonproline residues were in the disallowed regions. The extent of chemical-shift changes of U- and P-CPI-17 proteins ($\Delta\delta$) was calculated from the chemical shift value of proton (δ_H) and nitrogen (δ_N) in HSQC data by use of equation $\Delta\delta$ (chemical shift change) = $([\delta_H(U) - \delta_H(P)]^2 + 0.25[\delta_N(U) - \delta_N(P)]^2)^{1/2}$.

Structural Analysis

All structural images were drawn with MOLMOL (Koradi et al., 1996), Molscript (Kraulis, 1991), and Raster3D (Merrit and Bacon, 1997). Vector geometry mapping and calculations of surface potential and area were done by using an algorithm of Yap et al. (Yap et al., 2002) and PyMol Molecular Graphic System (http://www.pymol.org/), respectively. The rotation angle of A helix was estimated from mean value of differences on Calpha-Cbeta angle of each residue.

Phospho-Pivot Modeling

An in silico model of the ternary complex, P-T38-CPI-17/PP1 delta/MYPT1(1–299), was obtained by the phospho-pivot modeling method, as described previously (Matsuzawa et al., 2005a, 2005b). Structural data of P-T38-CPI-17 (present study) and the myosin phosphatase complex of MYPT1(1–299) and PP1 delta (Terrak et al., 2004) were used for the modeling. The best result was obtained when the phosphate group of P-CPI-17 was placed at a point 0.5 Å away from the putative phosphorus position. The atomic distance violation was set with the threshold of 3.5 Å (Ca-Ca) or 2.0 Å (N-O, N-N, O-O). Models without distance violation between main chain atoms, identified as 68 out of 186,624 models, were subjected to an energy minimization process with permitted of structural adjustments on both molecules, by using AMBER force field on SYBYL/BIOPOLYMER (Tripos, Inc.). In this modeling, atoms within 8 Å of CPI-17 were used for the energy calculation. The results of energy minimization are shown in Table S5. The orientation of P-CPI-17 against MYPT1•PP1 complex is the same in four of the best five models. Both electrostatic and hydrogen-bonding energy values dominantly contribute to the total binding force. The best model (shown in Figure 6A) includes 15 atomic violations.

Assays

CD spectrum measurements were performed on a JASCO 720 spectropolarimeter at various temperatures (20°C–95°C) with 20 μM U- and H6S-P-T38-CPI-17 full-length proteins in phosphate-buffered saline. Thermal stability of CPI-17 was assessed via the melting temperature (T_m) from the plot of molar ellipticity at 222 nm against the temperature. Other assays were carried out at 20°C. The H6S-tag does not affect the CD spectrum (data not shown). The inhibitory potency of CPI-17 proteins was measured by using myosin phosphatase purified from pig aorta smooth muscle with 0.5 μM ^{32}P-labeled phospho-myosin light chain as a substrate, at 20°C (Eto et al., 2003). The Ca^{2+} sensitizing effect of CPI-17 protein was examined at 20°C in vas deferens smooth-muscle strips permeabilized with beta-escin (Masuo et al., 1994). This tissue preparation includes a minimum amount of endogenous CPI-17 but retains other regulatory proteins, such as myosin phosphatase, PKC, and ROCK (Woodsome et al., 2001). Binding assay of P-CPI-17 was performed with synthetic segments of MYPT1(1–19) and MYPT1(24–41) (GenScript, Piscataway, NJ). MYPT1(1–19) and MYPT1(24–41) peptides were immobilized onto Sulfo-link beads (Pierce) via a C-terminal Cys residue added for crosslinking, and then excess reactive groups on the beads were quenched with 50 mM L-Cys. Blank beads for controls were treated with 50 mM L-Cys without peptide conjugation. H6S-P-T38-CPI-17 (0.1 μM) was mixed for 30 min at 23°C, with 10 μl of slurry in 150 μl of buffer A (50 mM MOPS-NaOH [pH 7.0] including 0.1 M NaCl, 1 mM EGTA, 0.1% Tween 20, 5% glycerol, 0.4 mM Pefabloc, and 0.5 mM TCEP). The beads were washed three times with 100 μl of buffer A, and bound CPI-17 was detected by immunoblotting with anti-CPI-17 by using FluoroChemSP CCD imaging system (AlphaInnotech). Relative amount of bound CPI-17 was obtained from three independent experiments by quantifying the band intensity with AlphaEace FC imaging software. Pull-down assay of myc-MYPT1•PP1 complex was performed by the method described previously (Eto et al., 2004). Briefly, HEK293 cells (60 mm dish) in Dulbecco's modified eagle medium supplemented with 10% fetal bovine serum (Mediatech, VA) were transiently transfected for 24 hr with 3.5 μg of myc-MYPT1(1–300) or myc- MYPT1(18–300) vector plus 0.5 μg of HA-PP1 delta vector with FuGENE6 transfection reagent (Roche). Empty vector without insert DNA were used as negative control. Cells were scraped off with 0.5 ml of buffer A and incubated for 10 min on ice. The homogenate was clarified by centrifugation for 10 min at 20,000 × g. The lysates were subjected to pull-down assay with thiophospho-CPI-17 beads. Thiophospho-CPI-17 was coupled with S-protein beads though S-tag sequence in the recombinant protein (Eto et al., 2004). After washing the beads, proteins bound to the beads were eluted with 30 μl of Laemmli buffer, and the samples were subjected to immunoblotting with anti-myc antibody (9E10). Staining intensity of myc-MYPT1 peptide was quantified by densitometry, described above.

Supplemental Data

Supplemental Data include phosphorylation of CPI-17(22–120) (Figure S1), zoomed HQSC spectrum (Figure S2), NOESY spectrum (Figure S3), heteronuclear NOE (Figure S4), statistics for NMR structure (Table S1), comparison of helix region between unphospho and phospho forms (Table S2), interhelical angles and distances (Table S3), phosphorylation of CPI-17 mutants (Table S4), and binding energy of P-CPI-17 and MYPT1•PP1 complex (Table S5) and are available at http://www.structure.org/cgi/content/full/15/12/1591/DC1/.

ACKNOWLEDGMENTS

This work was supported in part by a grant from Center for Nano Materials and Technology, Japan Advanced Institute of Science and Technology (to S.O.), National Heart Lung Blood Institute HL070881 (to T.K.), National Institute of General Medical Sciences GM56362 (to D.L.B.), and a Scientist Development Grant from the American Heart Association, C.U.R.E. grant from PA Department of Health, and National Heart Lung Blood Institute HL083261 (to M.E.). Drs. Eto and Brautigan have consultant agreements with Upstate/Millipore Co.

Received: April 23, 2007
Revised: October 2, 2007
Accepted: October 3, 2007
Published: December 11, 2007

REFERENCES

Bax, A., and Pochapsky, S.S. (1992). Optimized recording of heteronuclear multidimensional NMR spectra using pulsed field gradients. J. Magn. Reson. *99*, 638–643.

Bonnevier, J., and Arner, A. (2004). Actions downstream of cyclic GMP/protein kinase G can reverse protein kinase C-mediated phosphorylation of CPI-17 and Ca(2+) sensitization in smooth muscle. J. Biol. Chem. *279*, 28998–29003.

Brunger, A.T., Adams, P.D., Clore, G.M., DeLano, W.L., Gros, P., Grosse-Kunstleve, R.W., Jiang, J.S., Kuszewski, J., Nilges, M., Pannu, N.S., et al. (1998). Crystallography & NMR system: a new software suite for macromolecular structure determination. Acta Crystallogr. D Biol. Crystallogr. *54*, 905–921.

Byeon, I.J., Li, H., Song, H., Gronenborn, A.M., and Tsai, M.D. (2005). Sequential phosphorylation and multisite interactions characterize specific target recognition by the FHA domain of Ki67. Nat. Struct. Mol. Biol. *12*, 987–993.

Canagarajah, B.J., Khokhlatchev, A., Cobb, M.H., and Goldsmith, E.J. (1997). Activation mechanism of the MAP kinase ERK2 by dual phosphorylation. Cell *90*, 859–869.

Chang, S., Hypolite, J.A., DiSanto, M.E., Changolkar, A., Wein, A.J., and Chacko, S. (2006). Increased basal phosphorylation of detrusor smooth muscle myosin in alloxan-induced diabetic rabbit is mediated

by upregulation of ρ-kinase β and CPI-17. Am. J. Physiol. Renal Physiol. *290*, F650–F656.

Connor, J.H., Weiser, D.C., Li, S., Hallenbeck, J.M., and Shenolikar, S. (2001). Growth arrest and DNA damage-inducible protein GADD34 assembles a novel signaling complex containing protein phosphatase 1 and inhibitor 1. Mol. Cell. Biol. *21*, 6841–6850.

Dakshinamurti, S., Mellow, L., and Stephens, N.L. (2005). Regulation of pulmonary arterial myosin phosphatase activity in neonatal circulatory transition and in hypoxic pulmonary hypertension: a role for CPI-17. Pediatr. Pulmonol. *40*, 398–407.

Delaglio, F., Grzesiek, S., Vuister, G.W., Zhu, G., Pfeifer, J., and Bax, A. (1995). NMRPipe: a multidimensional spectral processing system based on UNIX pipes. J. Biomol. NMR *6*, 277–293.

Dimopoulos, G.J., Semba, S., Kitazawa, K., Eto, M., and Kitazawa, T. (2007). Ca^{2+}-dependent rapid Ca^{2+} sensitization of contraction in arterial smooth muscle. Circ. Res. *100*, 121–129.

Endo, S., Zhou, X., Connor, J., Wang, B., and Shenolikar, S. (1996). Multiple structural elements define the specificity of recombinant human inhibitor-1 as a protein phosphatase-1 inhibitor. Biochemistry *35*, 5220–5228.

Erdodi, F., Kiss, E., Walsh, M.P., Stefansson, B., Deng, J.T., Eto, M., Brautigan, D.L., and Hartshorne, D.J. (2003). Phosphorylation of protein phosphatase type-1 inhibitory proteins by integrin-linked kinase and cyclic nucleotide-dependent protein kinases. Biochem. Biophys. Res. Commun. *306*, 382–387.

Eto, M., Ohmori, T., Suzuki, M., Furuya, K., and Morita, F. (1995). A novel protein phosphatase-1 inhibitory protein potentiated by protein kinase C. Isolation from porcine aorta media and characterization. J. Biochem. (Tokyo) *118*, 1104–1107.

Eto, M., Senba, S., Morita, F., and Yazawa, M. (1997). Molecular cloning of a novel phosphorylation-dependent inhibitory protein of protein phosphatase-1 (CPI17) in smooth muscle: its specific localization in smooth muscle. FEBS Lett. *410*, 356–360.

Eto, M., Karginov, A., and Brautigan, D.L. (1999). A novel phosphoprotein inhibitor of protein type-1 phosphatase holoenzymes. Biochemistry *38*, 16952–16957.

Eto, M., Bock, R., Brautigan, D.L., and Linden, D.J. (2002a). Cerebellar long-term synaptic depression requires PKC-mediated activation of CPI-17, a myosin/moesin phosphatase inhibitor. Neuron *36*, 1145–1158.

Eto, M., Elliott, E., Prickett, T.D., and Brautigan, D.L. (2002b). Inhibitor-2 regulates protein phosphatase-1 complexed with NimA-related kinase to induce centrosome separation. J. Biol. Chem. *277*, 44013–44020.

Eto, M., Leach, C., Tountas, N.A., and Brautigan, D.L. (2003). Phosphoprotein inhibitors of protein phosphatase-1. Methods Enzymol. *366*, 243–260.

Eto, M., Kitazawa, T., and Brautigan, D.L. (2004). Phosphoprotein inhibitor CPI-17 specificity depends on allosteric regulation of protein phosphathase-1 by regulatory subunits. Proc. Natl. Acad. Sci. USA *101*, 8888–8893.

Eto, M., Kirkbride, J.A., and Brautigan, D.L. (2005). Assembly of MYPT1 with protein phosphatase-1 in fibroblasts redirects localization and reorganizes the actin cytoskeleton. Cell Motil. Cytoskeleton *62*, 100–109.

Etter, E.F., Eto, M., Wardle, R.L., Brautigan, D.L., and Murphy, R.A. (2001). Activation of myosin light chain phosphatase in intact arterial smooth muscle during nitric oxide-induced relaxation. J. Biol. Chem. *276*, 34681–34685.

Garrett, D.S., Powers, R., Gronenborn, A.M., and Clore, G.M. (1991). A common sense approach to peak picking in two-, three-, and four-dimensional spectra using automatic computer analysis of contour diagrams. J. Magn. Reson. *95*, 214–220.

Hartshorne, D.J., Ito, M., and Erdodi, F. (2004). Role of protein phosphatase type 1 in contractile functions: myosin phosphatase. J. Biol. Chem. *279*, 37211–37214.

Hayashi, Y., Senba, S., Yazawa, M., Brautigan, D.L., and Eto, M. (2001). Defining the structural determinants and a potential mechanism for inhibition of myosin phosphatase by the protein kinase C-potentiated inhibitor protein of 17 kDa. J. Biol. Chem. *276*, 39858–39863.

Jin, H., Sperka, T., Herrlich, P., and Morrison, H. (2006). Tumorigenic transformation by CPI-17 through inhibition of a merlin phosphatase. Nature *442*, 576–579.

Johnson, L.N., Noble, M.E.M., and Owen, D.J. (1996). Active and inactive protein kinases: structural basis for regulation. Cell *85*, 149–158.

Kawano, Y., Fukata, Y., Oshiro, N., Amano, M., Nakamura, T., Ito, M., Matsumura, F., Inagaki, M., and Kaibuchi, K. (1999). Phosphorylation of myosin-binding subunit (MBS) of myosin phosphatase by ρ-kinase in vivo. J. Cell Biol. *147*, 1023–1038.

Kimura, K., Ito, M., Amano, M., Chihara, K., Fukata, Y., Nakafuku, M., Yamamori, B., Feng, J., Nakano, T., Okawa, K., et al. (1996). Regulation of myosin phosphatase by Rho and Rho-associated kinase (Rho-kinase). Science *273*, 245–248.

Kitazawa, T., Masuo, M., and Somlyo, A.P. (1991). G protein-mediated inhibition of myosin light-chain phosphatase in vascular smooth muscle. Proc. Natl. Acad. Sci. USA *88*, 9307–9310.

Kitazawa, T., Eto, M., Woodsome, T.P., and Brautigan, D.L. (2000). Agonists trigger G protein-mediated activation of the CPI-17 inhibitor phosphoprotein of myosin light chain phosphatase to enhance vascular smooth muscle contractility. J. Biol. Chem. *275*, 9897–9900.

Kleywegt, G.J., and Jones, T.A. (1998). Databases in protein crystallography. Acta Crystallogr. D Biol. Crystallogr. *54*, 1119–1131.

Koradi, R., Billeter, M., and Wuthrich, K. (1996). MOLMOL: a program for display and analysis of macromolecular structures. J. Mol. Graph. *14*, 51–55, 29–32.

Koyama, M., Ito, M., Feng, J., Seko, T., Shiraki, K., Takase, K., Hartshorne, D.J., and Nakano, T. (2000). Phosphorylation of CPI-17, an inhibitory phosphoprotein of smooth muscle myosin phosphatase, by ρ-kinase. FEBS Lett. *475*, 197–200.

Kraulis, P.J. (1991). MOLSCRIPT: a program to produce both detailed and schematic plots pf protein structures. J. Appl. Crystallogr. *24*, 946–950.

Landrieu, I., Lacosse, L., Leroy, A., Wieruszeski, J.M., Trivelli, X., Sillen, A., Sibille, N., Schwalbe, H., Saxena, K., Langer, T., et al. (2006). NMR analysis of a τ phosphorylation pattern. J. Am. Chem. Soc. *128*, 3575–3583.

Laskowski, R.A., Rullmannn, J.A., MacArthur, M.W., Kaptein, R., and Thornton, J.M. (1996). AQUA and PROCHECK-NMR: programs for checking the quality of protein structures solved by NMR. J. Biomol. NMR *8*, 477–486.

Lesage, B., Beullens, M., Pedelini, L., Garcia-Gimeno, M.A., Waelkens, E., Sanz, P., and Bollen, M. (2007). A complex of catalytically inactive protein phosphatase-1 sandwiched between Sds22 and inhibitor-3. Biochemistry *46*, 8909–8919.

Li, M., Satinover, D.L., and Brautigan, D.L. (2007). Phosphorylation and functions of inhibitor-2 family of proteins. Biochemistry *46*, 2380–2389.

MacDonald, J.A., Borman, M.A., Muranyi, A., Somlyo, A.V., Hartshorne, D.J., and Haystead, T.A.J. (2001). Identification of the endogenous smooth muscle myosin phophatase-associated kinase. Proc. Natl. Acad. Sci. USA *98*, 2419–2424.

Masuo, M., Readon, S., Ikebe, M., and Kitazawa, T. (1994). A novel mechanism for the Ca^{2+}-sensitizating effect of protein kinase C on vascular smooth muscle: inhibition of myosin light chain phosphatase. J. Gen. Physiol. *104*, 265–286.

Matsumura, F. (2005). Regulation of myosin II during cytokinesis in higher eukaryotes. Trends Cell Biol. *15*, 371–377.

Matsuzawa, F., Aikawa, S., Ohki, S., and Eto, M. (2005a). Phospho-pivot modeling predicts specific interactions of protein phosphatase-1 with a phospho-inhibitor protein CPI-17. J. Biochem. (Tokyo) *137*, 633–641.

Matsuzawa, F., Ohki, S., Aikawa, S., and Eto, M. (2005b). Computational simulation for interactions of nano-molecules: the phospho-pivot modeling algorithm for prediction of interactions between a phospho-protein and its receptor. Sci. Technol. Adv. Mater. *6*, 463–467.

Merrit, E.A., and Bacon, D.J. (1997). Raster 3D photorealistics molecular graphics. Methods Enzymol. *277*, 505–524.

Muranyi, A., MacDonald, J.A., Deng, J.T., Wilson, D.P., Haystead, T.A., Walsh, M.P., Erdodi, F., Kiss, E., Wu, Y., and Hartshorne, D.J. (2002). Phosphorylation of the myosin phosphatase target subunit by integrin-linked kinase. Biochem. J. *366*, 211–216.

Neyroz, P., Desdouits, F., Benfenati, F., Knutson, J.R., Greengard, P., and Girault, J.A. (1993). Study of the conformation of DARPP-32, a dopamine- and cAMP-regulated phosphoprotein, by fluorescence spectroscopy. J. Biol. Chem. *268*, 24022–24031.

Ohama, T., Hori, M., Sato, K., Ozaki, H., and Karaki, H. (2003). Chronic treatment with interleukin-1β attenuates contractions by decreasing the activities of CPI-17 and MYPT-1 in intestinal smooth muscle. J. Biol. Chem. *278*, 48794–48804.

Ohki, S., Eto, M., Kariya, E., Hayano, T., Hayashi, Y., Yazawa, M., Brautigan, D., and Kainosho, M. (2001). Solution NMR structure of the myosin phosphatase inhibitor protein CPI-17 shows phosphorylation-induced conformational changes responsible for activation. J. Mol. Biol. *314*, 839–849.

Ohki, S., Eto, M., Shimizu, M., Takada, R., Brautigan, D.L., and Kainosho, M. (2003). Distinctive solution conformation of phosphatase inhibitor CPI-17 substituted with aspartate at the phosphorylation-site threonine residue. J. Mol. Biol. *326*, 1539–1547.

Pang, H., Guo, Z., Su, W., Xie, Z., Eto, M., and Gong, M.C. (2005). ρA-ρ kinase pathway mediates thrombin- and U-46619-induced phosphorylation of a myosin phosphatase inhibitor, CPI-17, in vascular smooth muscle cells. Am. J. Physiol. Cell Physiol. *289*, C352–C360.

Sakai, H., Chiba, Y., Hirano, T., and Misawa, M. (2005). Possible involvement of CPI-17 in augmented bronchial smooth muscle contraction in antigen-induced airway hyper-responsive rats. Mol. Pharmacol. *68*, 145–151.

Senba, S., Eto, M., and Yazawa, M. (1999). Identification of trimeric myosin phosphatase (PP1M) as a target for a novel PKC-potentiated protein phosphatase-1 inhibitory protein (CPI17) in porcine aorta smooth muscle. J. Biochem. (Tokyo) *125*, 354–362.

Somlyo, A.P., and Somlyo, A.V. (2003). Ca^{2+} sensitivity of smooth muscle and nonmuscle myosin II: modulated by G proteins, kinases, and myosin phosphatase. Physiol. Rev. *83*, 1325–1358.

Sprang, S.R., Acharya, K.R., Goldsmith, E.J., Stuart, D.I., Varvill, K., Fletterick, R.J., Madsen, N.B., and Johnson, L.N. (1988). Structural changes in glycogen phosphorylase induced by phosphorylation. Nature *336*, 215–221.

Terrak, M., Kerff, F., Langsetmo, K., Tao, T., and Dominguez, R. (2004). Structural basis of protein phosphatase 1 regulation. Nature *429*, 780–784.

Terry-Lorenzo, R.T., Elliot, E., Weiser, D.C., Prickett, T.D., Brautigan, D.L., and Shenolikar, S. (2002). Neurabins recruit protein phosphatase-1 and inhibitor-2 to the actin cytoskeleton. J. Biol. Chem. *277*, 46535–46543.

Trinkle-Mulcahy, L., Ichikawa, K., Hartshorne, D.J., Siegman, M.J., and Butler, T. (1995). Thiophosphorylation of the 130-kDa subunit is associated with a decreased activity of myosin light chain phosphoatase in a-toxin-permeabilized smooth muscle. J. Biol. Chem. *270*, 18191–18194.

Wang, H., and Brautigan, D.L. (2002). A novel transmembrane Ser/Thr kinase complexes with protein phosphatase-1 and inhibitor-2. J. Biol. Chem. *277*, 49605–49612.

Woodsome, T.P., Eto, M., Everett, A., Brautigan, D.L., and Kitazawa, T. (2001). Expression of CPI-17 and myosin phosphatase correlates with Ca^{2+} sensitivity of protein kinase C-induced contraction in rabbit smooth muscle. J. Physiol. *535*, 553–564.

Xie, Z., Su, W., Guo, Z., Pang, H., Post, S.R., and Gong, M.C. (2006). Up-regulation of CPI-17 phosphorylation in diabetic vasculature and high glucose cultured vascular smooth muscle cells. Cardiovasc. Res. *69*, 491–501.

Yap, K.L., Ames, J.B., Swindells, M.B., and Ikura, M. (2002). Vector geometry mapping. A method to characterize the conformation of helix-loop-helix calcium-binding proteins. Methods Mol. Biol. *173*, 317–324.

Zhang, J., Zhang, F., Ebert, D., Cobb, M.H., and Goldsmith, E.J. (1995). Activity of the MAP kinase ERK2 is controlled by a flexible surface loop. Structure *3*, 299–307.

Accession Numbers

The atomic coordinates and the chemical shift table of P-T38-CPI-17(22–120) protein are deposited in the Protein Data Bank (2RLT) and BioMagResoBank (15428), respectively.

